Inorganic Chemistry

Article

pubs.acs.org/IC

Self-Assembly and Redox Modulation of the Cavity Size of an Unusual Rectangular Iron Thiolate Aryldiisocyanide Metallocyclophane

Pei-Chin Lin,[†] Hsing-Yin Chen,[†] Po-Yu Chen,[†] Ming-Hsi Chiang,[‡] Michael Y. Chiang,[§] Ting-Shen Kuo,[⊥] and Sodio C. N. Hsu*[,†]

[†]Department of Medicinal and Applied Chemistry, Kaohsiung Medical University, Kaohsiung 807, Taiwan

[‡]Institute of Chemistry, Academia Sinica, Nankang, Taipei 115, Taiwan

[§]Department of Chemistry, National Sun Yat-Sen University, Kaohsiung 804, Taiwan

[⊥]Department of Chemistry, National Taiwan Normal University, Taipei 116, Taiwan

Supporting Information

ABSTRACT: The decarbonylation reaction of ferric carbonyl dicationic $[Cp_2Fe_2(\mu\text{-SEt})_2(CO)_2](BF_4)_2$ [**1**$(BF_4)_2$] carried out in refluxing acetonitrile affords a binuclear iron−sulfur core complex $[Cp_2Fe_2(\mu\text{-SEt})_2(CH_3CN)_2](BF_4)_2$ [**2**$(BF_4)_2$] containing two acetonitrile coordinated ligands. The treatment of **2**$(BF_4)_2$ with 2 equiv of the 1,4-diisocyanobenzene (1,4-CNC_6H_4NC) results in the formation of the diisocyanide complex $[Cp_2Fe_2(\mu\text{-SEt})_2(1,4\text{-}CNC_6H_4NC)_2](BF_4)_2$ [**3**$(BF_4)_2$]. The rectangular tetranuclear iron thiolate aryldiisocyanide metallocyclophane complex $[Cp_4Fe_4(\mu\text{-SEt})_4(\mu\text{-}1,4\text{-}CNC_6H_4NC)_2](BF_4)_4$ [**4**$(BF_4)_4$] has been synthesized by a self-assembly reaction between equimolar amounts of **2**$(BF_4)_2$ and 1,4-diisocyanobenzene or by a stepwise route involving mixing of a 1:1 molar ratio of complexes **2**$(BF_4)_2$ and **3**$(BF_4)_2$. Chemical reduction of **4**$(BF_4)_4$ by KC_8 was observed to produce the reduction product **4**$(BF_4)_2$. The spectroscopic and electrochemical properties of the iron−sulfur core complexes **1**$(PF_6)_2$, **3**$(BF_4)_2$, **4**$(BF_4)_4$, and **4**$(BF_4)_2$ were determined. Finally, differences between the redox control cavities of rectangular tetranuclear iron thiolate aryldiisocyanide complexes are revealed by a comparison of the X-ray crystallographically determined structures of complexes **4**$(BF_4)_4$ and **4**$(BF_4)_2$.

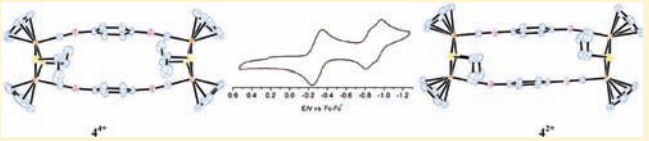

INTRODUCTION

During the past few decades, the development of methods for the self-assembly of metal-containing supramolecules and coordination polymers has attracted significant interest owing to the fact that these supramolecular structures possess unique functional properties and diverse applications in the fields of host−guest chemistry, redox reactivity, magnetic behavior, photo- and electrochemical sensing, and catalysis.[1−5] Stang and co-workers have generated a combinatorial library of members of this metal-containing supramolecular family that contain cyclic molecular polygon structures. This was accomplished by employing systematic combinations of building blocks that correspond to specific metal fragments with predetermined shapes and angles.[6] These workers observed that the half-sandwich metal fragment motif leads to strong suppression of polymerization reactions to such an extent that the resulting molecular assemblies form specific supramolecular structures.[7] By utilizing this approach, Rauchfuss et al. demonstrated that the organometallic half-sandwich Cp*Rh fragments can serve as building blocks in the construction of coordination cages linked by cyanide bridges.[8] Since that time, organometallic half-sandwich complexes (π-ligand)M [(π-ligand)M = (arene)Ru, CpCo, Cp*Co, Cp*Rh, Cp*Ir] have been widely used as building blocks for the construction of unique supramolecular architectures including metallocycles, rectangles, trigonal prisms, hexagonal prisms, and even helicates.[7,9−11]

Iron thiolate core complexes have significance because they are synthetic substances that mimick the redox behavior of active sites of metalloproteins, such as hydrogenase and ferredoxins.[12,13] Among synthetic iron thiolate complexes, dinuclear cyclopentadienyliron thiolate-bridged species are perhaps the most well-studied class from the perspective of their redox crystal structural properies.[14−29] However, these substances have seldom been used as building blocks in the construction of supramolecular complex building units. In a recent effort aimed at expanding the range of supramolecular structural motifs of tetrametallic organometallic half-sandwich complexes and continuing studies of dinuclear cyclopentadienyliron thiolate-bridged complexes and isocyanide (CNR) coordination chemistry,[30−33] we have investigated use of the iron thiolate core complex $\{Cp_2Fe_2(\mu\text{-SEt})_2\}$ as a syn-ligand-directed building unit for rectangular metallomacrocycle formation. Specifically, we felt that this substance would self-assemble with 1,4-diisocyanobenzene (1,4-CNC_6H_4NC), which is capable of serving as a bridging ligand between two metal centers, to form the coordination metallomacrocycles.[34−37]

Received: June 28, 2011
Published: October 14, 2011

Scheme 1. Synthesis of the Rectangular Iron Thiolate Aryldiisocyanide Metallocyclophane 4^{4+} and Its Reduced Analogue 4^{2+}

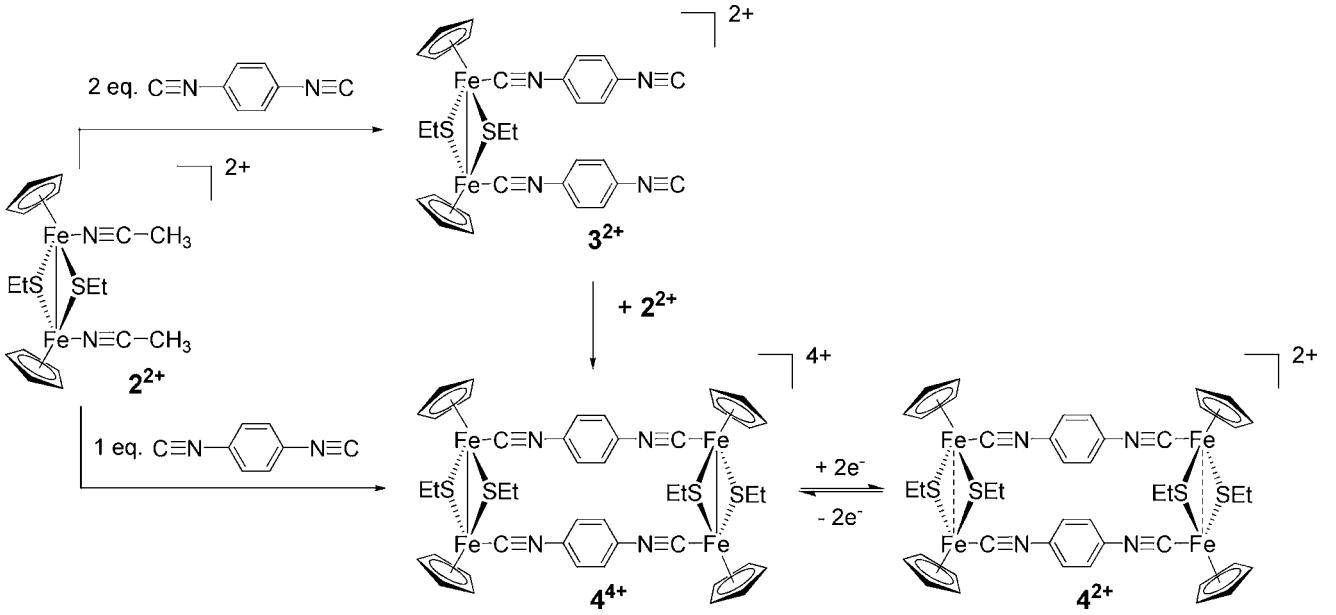

Below, we describe the results of this study, which has resulted in the development of stepwise and direct self-assembly routes for construction of rectangular macrocyclic iron thiolate core complexes $\{Cp_2Fe_2(\mu\text{-}SEt)_2\}$ bridged by 1,4-diisocyanobenzene ligands. The concept of cavity modulation control of the electrochemical properties of the rectangular iron thiolate aryldiisocyanide metallocyclophane was demonstrated by utilizing X-ray crystallographic and electrochemical techniques. In addition, the solid-state structures of these dinuclear cyclopentadienyliron thiolate-bridged complexes with or without bridged diisocyanide ligands were also analyzed.

RESULTS AND DISCUSSION

Synthesis and Spectroscopic Studies. Chemical oxidation of the binuclear iron thiolate core complex $Cp_2Fe_2(\mu\text{-}SEt)_2(CO)_2$ with bromine led to formation of the dicationic ferric carbonyl species $[Cp_2Fe_2(\mu\text{-}SEt)_2(CO)_2]^{2+}$ ($\mathbf{1}^{2+}$), which was isolated as its BF_4^- or PF_6^- salt.[25] Ferric carbonyl species of this type are unusual in that only a few examples have been prepared and characterized previously.[38−43] The complex $[Cp_2Fe_2(\mu\text{-}SEt)_2(CH_3CN)_2](BF_4)_2$ [$\mathbf{2}(BF_4)_2$] was generated by reaction of the dicationic ferric carbonyl substance $\mathbf{1}^{2+}$ with excess NH_4BF_4 in refluxing acetonitrile.[20] The treatment of $\mathbf{2}(BF_4)_2$ with 2 equiv of 1,4-CNC_6H_4NC led to formation of the diisocyanide adduct $[Cp_2Fe_2(\mu\text{-}SEt)_2(1,4\text{-}CNC_6H_4NC)_2](BF_4)_2$ [$\mathbf{3}(BF_4)_2$] in an essentially quantitative yield. According to the results of previous studies, it is expected that $\mathbf{2}(BF_4)_2$ would participate in a syn-type substitution of an acetonitrile ligand.[30] In fact, the reaction of $\mathbf{3}(BF_4)_2$ with an equimolar amount of $\mathbf{2}(BF_4)_2$ produces the rectangular tetranuclear complex $[Cp_4Fe_4(\mu\text{-}SEt)_4(\mu\text{-}1,4\text{-}CNC_6H_4NC)_2](BF_4)_4$ [$\mathbf{4}(BF_4)_4$]. In contrast, the treatment of $\mathbf{2}(BF_4)_2$ with an equimolar amount of 1,4-CNC_6H_4NC also generates the rectangular tetranuclear complex $\mathbf{4}(BF_4)_4$. Finally, reduction of $\mathbf{4}(BF_4)_4$ using 2 equiv of KC_8 was employed to produce the desired two-electron-reduced species $[Cp_4Fe_4(\mu\text{-}SEt)_4(\mu\text{-}1,4\text{-}CNC_6H_4NC)_2](BF_4)_2$ [$\mathbf{4}(BF_4)_2$]. The chemical reactions described above are summarized in Scheme 1.

The ^1H and $^{13}C\{^1H\}$ NMR spectra of $\mathbf{1}(BF_4)_2$, $\mathbf{3}(BF_4)_2$, and $\mathbf{4}(BF_4)_4$ contain several sharp lines that indicate that these substances are diamagnetic and, as a result, they possess Fe—Fe single bonds. In addition, the ^1H NMR spectra of these complexes contain only one set of Cp signals with chemical shifts in the 5.0−6.0 ppm range and ethylthiolate resonances at ca. 3.0 (quartet) and 1.8 (triplet) ppm. The ^1H NMR spectrum of $\mathbf{3}(BF_4)_2$ exhibits a well-separated AA′BB′ pattern corresponding to the arene ring protons, which is characteristic of the presence of two distinctly different iron-coordinated and free coordination environments of the isocyanide moieties in the 1,4-diisocyanobenzene bridging ligand. In contrast, the ^1H NMR spectrum of $\mathbf{4}(BF_4)_4$ contains only one resonance for protons on the 1,4-diisocyanobenzene ring, showing that this ligand exists in a centrosymmetrical environment in this complex. The $^{13}C\{^1H\}$ NMR spectrum of $\mathbf{3}(BF_4)_2$, in contrast to that of $\mathbf{4}(BF_4)_4$, contains two signals in the CNR region that are consistent with the presence of two different coordinated environments. The ^1H NMR spectrum of the two-electron-reduced species arising from $\mathbf{4}(BF_4)_2$ does not contain resonances in the diamagnetic region, thereby indicating that it is paramagnetic species. In addition, reduced $\mathbf{4}(BF_4)_2$ has a magnetic moment of 2.75 μ_B (determined by using Evans' method[44,45] on an acetonitrile solution at 25 °C), which is in the expected range for spin-only magnetic moments for a substance containing two unpaired electrons (triplet spin state; 2.83 μ_B).

The positive-mode electrospray ionization mass spectrometry [ESI-MS(+)] data for the binuclear complexes $\mathbf{1}(BF_4)_2$ and $\mathbf{3}(BF_4)_2$ and the tetranuclear complex $\mathbf{4}(BF_4)_2$ show the presence of 2+ charged molecular ion peaks and corresponding fragment ion peaks at m/z 212.00, 310.04, and 492.26, respectively. A 4+ charged ion is also observed in the ESI-MS(+) spectrum of the tetranuclear complex $\mathbf{4}(BF_4)_4$. The pattern of the resolved signals centered at m/z 246.05 corresponding to $[M]^{4+}$ is in close agreement with the theoretically predicted isotope abundance pattern. The ν_{CO} bands at 2071 (s) and 2059 (m) cm^{-1} for the ferric carbonyl groups in $\mathbf{1}(BF_4)_2$ are ca. 116 and 59 cm^{-1} larger than those of

dx.doi.org/10.1021/ic201380k | Inorg. Chem. 2011, 50, 10825−10834

the ferrous carbonyl groups in the respective complex $Cp_2Fe_2(\mu\text{-SEt})_2(CO)_2$ [1955(s) and 1926(m) cm^{-1}][23] and the mixed-valence analogue $[Cp_2Fe_2(\mu\text{-SEt})_2(CO)_2]^+$ [2012(s) and 1990(m) cm^{-1}].[25] The CNR stretching frequencies of $\mathbf{3}(BF_4)_2$ appear at 2164(s) and 2128(m) cm^{-1} for the coordinated and uncoordinated isocyanide functional groups, respectively. These values are in agreement with data arising from crystallographic analysis. Although the isocyanide and carbonyl (CO) ligands are isoelectronic, their bonding modes are distinctly different.[46] The CO ligand is a stronger π acceptor and a weaker σ donor that stabilizes low-oxidation-state transition-metal ions. These properties result in a weakening of the CO bond and a decrease of the carbonyl stretching frequency in ligated CO complexes in contrast to that of the free ligand.[47] On the other hand, isocyanides are stronger σ donors and poorer π acceptors than CO.[32,33,46−48] The CNR stretching frequency generally occurs above that of the free ligand, implying that the dominant mode of bonding involves σ donation with only a minor contribution from π-acceptor interactions in metal isocyanide complexes.[32−37,46−49] In contrast with $\mathbf{3}(BF_4)_2$, only one ν_{CNR} at 2156 cm^{-1} is seen for $\mathbf{4}(BF_4)_4$, indicating that it is a rectangular tetranuclear complex in a manner that is consistent with the presence of the homonuclear bridging diisocyanide ligand (Figure 1). In

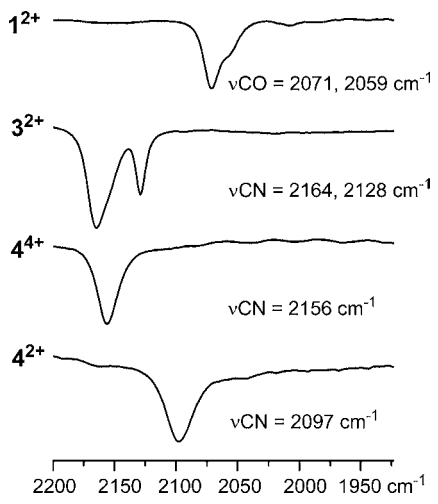

Figure 1. FT-IR spectra (CH_3CN solution) in the CO and CN regions of $\mathbf{1}(BF_4)_2$, $\mathbf{3}(BF_4)_2$, $\mathbf{4}(BF_4)_4$, and $\mathbf{4}(BF_4)_2$.

addition, two-electron-reduced $\mathbf{4}(BF_4)_2$ (2097 cm^{-1}) displays a 59 cm^{-1} lower CNR stretching frequency in contrast to the parent $\mathbf{4}(BF_4)_4$. The decreased CNR stretching frequency suggests that the π-acceptor contribution of the ligand is increased when the iron core of the tetranuclear iron thiolate core system is reduced.

Electrochemistry. Only a few redox-active metallosupramolecular complexes have been recently identified and discussed by van Koten et al. and others.[2,50,51] Our examination of the electrochemical reduction of $\mathbf{3}(BF_4)_2$ in acetonitrile by utilizing cyclic voltammetry (CV) shows that this complex exhibits two reversible waves at −0.308 and −0.848 V (Figure 2a). This observation indicates that no significant structural reorganization occurs during the redox processes of $\mathbf{3}(BF_4)_2$. The two redox processes are well separated, and the potential difference of $E_{1/2}^{Red1} - E_{1/2}^{Red2}$ (ΔE = 0.540 V) of $\mathbf{3}(BF_4)_2$ is attributed to strong exchange interactions between the two Fe

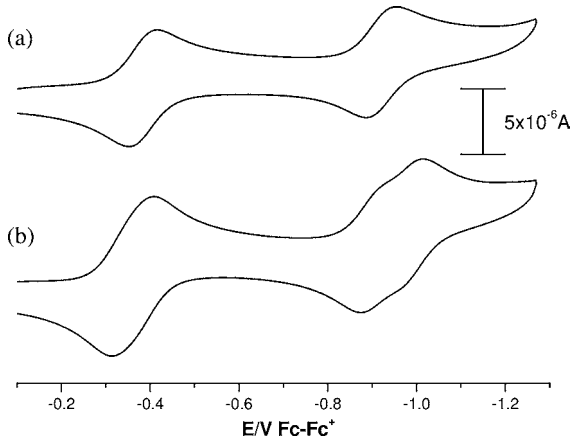

Figure 2. CV spectra of (a) $\mathbf{3}(BF_4)_2$ in CH_3CN (2×10^{-4} M) and (b) $\mathbf{4}(BF_4)_4$ in CH_3CN (2×10^{-4} M). Scan rate = 100 mV s^{-1}; electrolyte = $(Bu_4N)(PF_6)$ (0.1 M).

centers that $\mathbf{3}(BF_4)_2$ propagated through the orbitals of the metal−metal bond and the bridged thiolate ligands. Similar electrochemical studies with related thiolate-bridged CpFe complexes have led to the same conclusion (Table 1).[14,21,30]

Diisocyanide ligands, such as 1,4-diisocyanobenzene, are able to participate in structural and electronic bridges between two metal-ion centers and, consequently, assist electron communication and even transfer through the metal−ligand−metal frameworks.[48,49] Therefore, the electrochemical reduction of $\mathbf{4}(BF_4)_4$ was examined in order to compare its redox properties with those of $\mathbf{3}(BF_4)_2$. Reduction of $\mathbf{4}(BF_4)_4$ is revealed by the presence of three fully reversible reduction waves (Figure 2b), the first of which might correspond to the two independent iron thiolate core $[Cp_2Fe_2(\mu\text{-SEt})_2]^{2+/+}$ ($\mathbf{4}^{4+/2+}$; $Fe^{III}Fe^{III}$═$Fe^{III}Fe^{III}$ to $Fe^{II}Fe^{III}$═$Fe^{II}Fe^{III}$; Scheme 2) redox couple ($E_{1/2}^{Red1}$ = −0.280 V). This wave is 2 times more intense than those corresponding to the two other overlapping reversible redox processes ($E_{1/2}^{Red2}$ = −0.836 V and $E_{1/2}^{Red3}$ = −0.930 V). These features can be assigned to the respective $\mathbf{4}^{2+/+}$ ($Fe^{II}Fe^{III}$═$Fe^{II}Fe^{III}$ to $Fe^{II}Fe^{II}$═$Fe^{II}Fe^{III}$) and $\mathbf{4}^{+/0}$ ($Fe^{II}Fe^{II}$═$Fe^{II}Fe^{III}$ to $Fe^{II}Fe^{II}$═$Fe^{II}Fe^{II}$) redox couples. A graphical simulation (COOL algorithm)[52] of the CV profile is shown in Figure S11 (Supporting Information). Because the reduction potentials of $\mathbf{4}(BF_4)_4$ are close to those of $\mathbf{3}(BF_4)_2$, it is reasonable to conclude that the electronic environments of the Fe centers are only slightly perturbed when a molecular square is formed. The first two-electron reduction couple of $\mathbf{4}(BF_4)_4$ is shifted slightly in the positive direction in a manner similar to that of $\mathbf{3}(BF_4)_2$. Furthermore, the identical iron thiolate core environment in $\mathbf{3}(BF_4)_2$ is associated with two separate one-electron redox events for each of the Fe centers, which contrasts with that of $\mathbf{4}(BF_4)_4$, where one two-electron redox event occurs.

The strikingly unique CV properties of $\mathbf{4}(BF_4)_4$ appear to show that the 1,4-diisocyanobenzene ligand does not act as a molecular wire to convey electrons from one iron thiolate core $\{Cp_2Fe_2(\mu\text{-SEt})_2\}$ to another in the ferric state. Furthermore, it is possible that the bridged 1,4-diisocyanobenzene ligand serves as a molecular wire to transfer electrons between the sides of the diiron thiolate core during the third reduction process. The small potential difference of $E_{1/2}^{Red2} - E_{1/2}^{Red3}$ (ΔE = 0.094 V) observed for $\mathbf{4}(BF_4)_4$ can be attributed to the existence of weak exchange interactions between the two iron thiolate core

dx.doi.org/10.1021/ic201380k | Inorg. Chem. 2011, 50, 10825−10834

Table 1. CV Data and Comproportionation Constants for Iron Thiolate Core Complexes in MeCN−[NBu$_4$](PF$_6$)[a]

complex	$E_{1/2}^{Red1}$	$E_{1/2}^{Red2}$	$E_{1/2}^{Red3}$	ΔE	K_{com}[c]	ref
$[Cp_2Fe_2(\mu\text{-SEt})_2(CN)(CNMe)]^+$	−0.836	−1.545		0.709	9.92×10^{11}	30
$[Cp_2Fe_2(\mu\text{-SEt})_2(CNMe)_2]^{2+}$	−0.525	−1.164		0.639	6.49×10^{10}	30
$[Cp_2Fe_2(\mu\text{-SR})_2(MeCN)_2]^{2+}$ ($\mathbf{2}^{2+}$)	−0.605	−1.028 (irr)				30
$[Cp_2Fe_2(\mu\text{-SEt})_2(1,4\text{-}CNC_6H_4NC)_2]^{2+}$ ($\mathbf{3}^{2+}$)	−0.308	−0.848		0.540	1.37×10^9	this work
$[Cp_4Fe_4(\mu\text{-SEt})_4(\mu\text{-}1,4\text{-}CNC_6H_4NC)_2]^{4+}$ ($\mathbf{4}^{4+}$)	−0.280	−0.836	−0.930	0.556	2.57×10^9	this work
				0.094	3.89×10^1	

[a]Potentials (in V vs Fc$^+$/Fc) were measured at a glassy carbon electrode at a scan rate of 0.1 V s^{-1}. [b]Quasi-reversible. [c]ΔE = 0.0591 log K_{com}.

Scheme 2. Representation of the Oxidation State Changes of Iron in the Tetranuclear Complex 4^{4+} in the Electrochemical Processes[a]

$$Fe^{III}Fe^{III}{=}Fe^{III}Fe^{III}\ (\mathbf{4}^{4+}) \underset{-2e^-}{\overset{+2e^-}{\rightleftharpoons}} Fe^{II}Fe^{III}{=}Fe^{II}Fe^{III}\ (\mathbf{4}^{2+}) \underset{-e^-}{\overset{+e^-}{\rightleftharpoons}} Fe^{II}Fe^{II}{=}Fe^{II}Fe^{III}\ (\mathbf{4}^{+}) \underset{-e^-}{\overset{+e^-}{\rightleftharpoons}} Fe^{II}Fe^{II}{=}Fe^{II}Fe^{II}\ (\mathbf{4})$$

[a]The = symbols represent the bridged 1,4-diisocyanobenzene ligands.

{Cp$_2$Fe$_2$(μ-SEt)$_2$}, which is bridged by the 1,4-diisocyanobenzene ligand.

The electrochemical behavior observed for $\mathbf{4}(BF_4)_4$ is similar to those seen with other cationic rectangular complexes.[53,54] However, $\mathbf{4}(BF_4)_4$ is unique in that it contains metal−metal bonding that is different from the types of structure compositions of other cationic rectangular complexes explored.[53,54] By using the $E_{1/2}$ values determined for the redox couples, comproportionation constants, K_{com},[55] for the iron thiolate core complexes {Cp$_2$Fe$_2$(μ-SEt)$_2$} were calculated (Table 1). The larger value of K_{com} suggests that the mixed-valence-reduced $\mathbf{4}(BF_4)_2$ will be thermodynamically stable. Indeed, the ability to isolate the two-electron-reduced product $\mathbf{4}(BF_4)_2$ supports the proposed electroredox behavior of this substance displayed in Scheme 2. Furthermore, the CV spectrum of $\mathbf{4}(BF_4)_2$ contains the same oxidative and reductive waves that are present in the spectrum of $\mathbf{4}(BF_4)_4$ (Figure S11 in the Supporting Information).

Molecular Structures of $\mathbf{1}(PF_6)_2$, $\mathbf{3}(BF_4)_2$, $\mathbf{4}(BF_4)_4$, and $\mathbf{4}(BF_4)_2$. Interestingly, the results of only spectroscopic studies of the dicationic ferric carbonyl complex $\mathbf{1}(PF_6)_2$ have been described thus far.[25] Because not many ferric carbonyl complexes are known[38−43] and only a few have been subjected to crystallographic analysis,[14] we have carried out an investigation of probing a comparison of the molecular structure of complex $\mathbf{1}(PF_6)_2$ with other known ferrous carbonyl analogues including Cp$_2$Fe$_2$(μ-SEt)$_2$(CO)$_2$,[17] $\mathbf{3}(BF_4)_2$, and $\mathbf{4}(BF_4)_4$. The crystallographic results of the two-electron-reduced product $\mathbf{4}(BF_4)_2$ have also been compared with those of its precursor $\mathbf{4}(BF_4)_4$. The results of crystallographic analyses demonstrate that $\mathbf{1}(PF_6)_2$ and $\mathbf{3}(BF_4)_2$ have dinuclear nature and that $\mathbf{4}(BF_4)_4$ and $\mathbf{4}(BF_4)_2$ are tetranuclear. The crystal units of $\mathbf{4}(BF_4)_4$ and $\mathbf{4}(BF_4)_2$ consist of molecular arrays with a crystallographically imposed inversion center in the middle of the Fe1···Fe1^i vector. Solvent acetonitrile molecules are present in the crystal units of $\mathbf{4}(BF_4)_4$ and $\mathbf{4}(BF_4)_2$ on the outside of the square framework. ORTEP plots of the crystal structures of $\mathbf{1}(PF_6)_2$, $\mathbf{3}(BF_4)_2$, $\mathbf{4}(BF_4)_4$, and $\mathbf{4}(BF_4)_2$ are displayed in Figures 3−6, respectively, and selected bond distances and angles are shown in Table 2.

Complexes $\mathbf{1}(PF_6)_2$ and $\mathbf{3}(BF_4)_2$ both contain CpFe units in cis relative configurations bridged by two ethylthiolate ligands, with the substituents adopting a syn orientation with respect to one another but anti with respect to the Cp ligands. The CO or

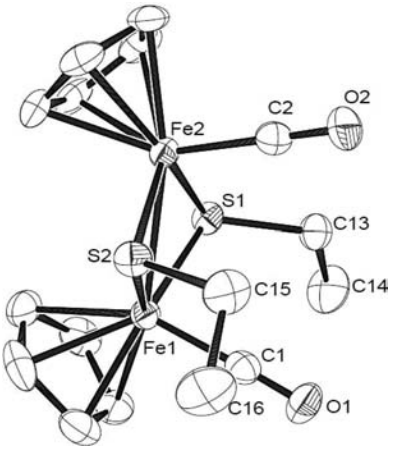

Figure 3. ORTEP representation of the crystal structure of the cation of $\mathbf{1}(PF_6)_2$ (50% ellipsoid; all H atoms, anions, and solvent molecules are omitted for clarity).

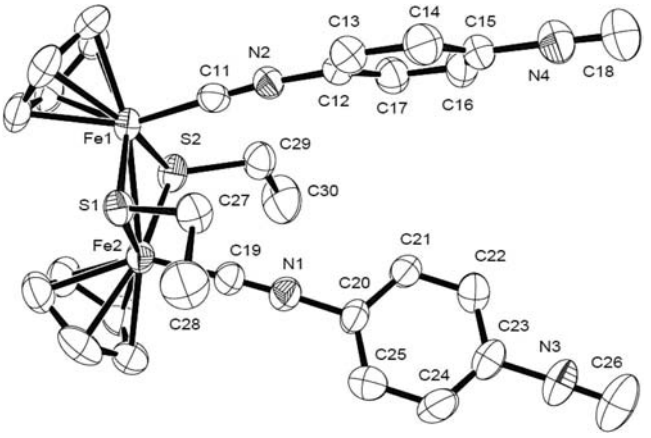

Figure 4. ORTEP representation of the crystal structure of the cation of $\mathbf{3}(BF_4)_2$ (50% ellipsoid; all H atoms, anions, and solvent molecules are omitted for clarity).

diisocyanide ligands occupy the remaining coordination sites. The Fe−CO [1.797(6) and 1.804(6) Å] and C−O [1.123(6) and 1.130(6) Å] distances in the ferric carbonyl complex $\mathbf{1}(PF_6)_2$ are longer and shorter, respectively, than those in the iron(II) analogue Cp$_2$Fe$_2$(μ-SEt)$_2$(CO)$_2$.[17] This finding in-

dx.doi.org/10.1021/ic201380k | Inorg. Chem. 2011, 50, 10825−10834

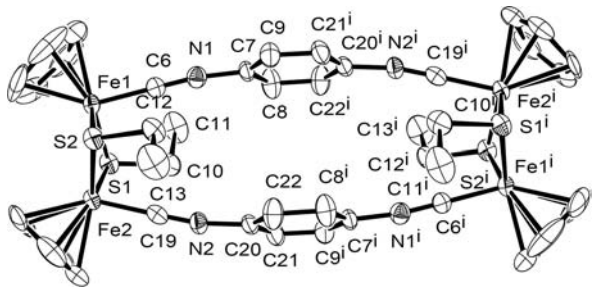

Figure 5. ORTEP representation of the crystal structure of the cation of $4(BF_4)_4$ (50% ellipsoid; all H atoms, anions, and solvent molecules are omitted for clarity).

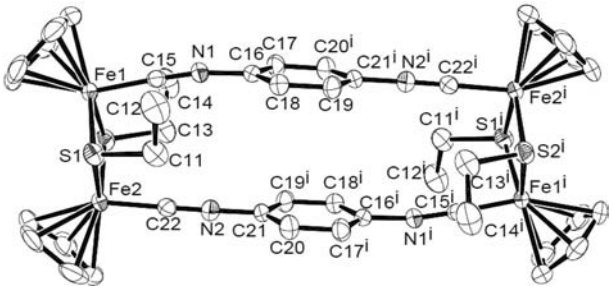

Figure 6. ORTEP representation of the crystal structure of the cation of $4(BF_4)_2$ (50% ellipsoid; all H atoms, anions, and solvent molecules are omitted for clarity).

dicates that the oxidation state of the metal center influences bond distances owing to the π-back-bonding ability of CO. On the other hand, this ability has only a slight effect on the Fe–CNR distances [$4(BF_4)_4$, 1.830(6) and 1.843(6) Å; $4(BF_4)_2$, 1.812(4) and 1.809(4) Å], and it does not significantly perturb the C–N distances [$4(BF_4)_4$, 1.830(6) and 1.843(6) Å; $4(BF_4)_2$, 1.812(4) and 1.809(4) Å]. These observations suggest again that a minor π-acceptor contribution exists between the Fe cation and C atom of the 1,4-diisocyanobenzene ligand in the tetranuclear iron–sulfur core system. Complex $4(BF_4)_4$ has an iron core geometry similar to those of $1(PF_6)_2$ and $3(BF_4)_2$ except that in the former complex the two ethylthiolate ligands adopt an anti orientation. On the other hand, the structure of $4(BF_4)_2$ is similar to those of $1(PF_6)_2$ and $3(BF_4)_2$ but different from that of $4(BF_4)_4$ with respect to the syn orientation of the ethylthiolate ligands.

The Fe–S distances in the structures of $1(PF_6)_2$, $3(BF_4)_2$, and $4(BF_4)_4$ fall in the range of 2.19–2.23 Å, values that are comparable to those of other thiolate-bridged, iron(III)-containing diiron-centered complexes.[14,21,30] The distances in $1(PF_6)_2$, which are close to those in the known iron carbonyl analogues, increase in the order $\mathbf{1}^{2+}$ (average 2.2060 Å) < $[Cp_2Fe_2(\mu\text{-SEt})_2(CO)_2]^+$ (average 2.240 Å)[19] < $Cp_2Fe_2(\mu\text{-SEt})_2(CO)_2$ (average 2.2710 Å).[17] A similar trend is also observed for the longer distances of the reduced product $4(BF_4)_2$ (average 2.2432 Å) and the shorter distances of $4(BF_4)_4$ (average 2.2112 Å). The results appear to reflect varying bonding interactions between different iron oxidation states and the thiolate-bridged donors. The respective Fe–Fe distances in $1(PF_6)_2$, $3(BF_4)_2$, and $4(BF_4)_4$ of 2.6444(10), 2.6309(11), and 2.6596(11) Å agree well with the values observed for ferric $[Cp_2Fe_2(\mu\text{-SEt})_2(NCMe)_2]^{2+}$ and other related complexes,[14,21,30] which typically fall in the characteristic two-electron Fe–Fe bond range of 2.5–2.8 Å. A longer Fe–Fe distance is observed in the reduced product $4(BF_4)_2$ [2.9706(8) Å], in which the one-electron Fe–Fe bond is proposed to exist. This finding agrees with distances seen in other known iron thiolate core complexes $\{Cp_2Fe_2(\mu\text{-SEt})_2\}$ containing the same Fe–Fe bonding feature.[15,19,27]

Fe–Fe Distance and Cavity Modulation. A comparison of the geometries of the iron–sulfur core complexes $\{Cp_2Fe_2(\mu\text{-SEt})_2\}$ containing CO or isocyanide ligands clearly illustrates that Fe–Fe distances are reflective of the oxidation states of the core irons. This behavior is also paralleled by both a substantial drop in the Fe–Fe distance and a large Fe–S–Fe distortion angle, as exemplified by the data presented in Scheme 3 and Table 2. This bond lengthening is accompanied by an increase (of ca. 9°) in the Fe–S–Fe angle. Still longer nonbonded Fe–Fe distances of 3.4 Å are present in comparable iron(II) complexes,[17] and these are associated with ca. 16° further widening of the Fe–S–Fe angles to 97–100° (Table 2). A comparison of the structural features of $4(BF_4)_4$ and the reduced product $4(BF_4)_2$ also follows the trends summarized above. These findings can be rationalized in terms of the reversible addition of one or two electrons to the σ-antibonding orbital of $(Fe^{III}SEt)_2$ or the removal of electrons from the σ-antibonding orbital of $(Fe^{II}SEt)_2$.[21,30,56] Therefore, the longer Fe–Fe bond distance exists in the paramagnetic product $4(BF_4)_2$, for which a one-electron Fe–Fe bond is proposed. Similar structural features have been observed for the related thiolate-bridged CpFe complexes also containing one-electron Fe–Fe bonds.[15,19,27]

A comparison of $4(BF_4)_4$ with that of the reduced product $4(BF_4)_2$ shows that the cation complex $4(BF_4)_4$ has a smaller rectangular cavity with dimensions of 2.66 × 11.35 Å, as defined by the Fe centers that are bridged by four S atoms of the ethylthiolate ligands and two diisocyanide molecules (Scheme 4). The reduced complex $4(BF_4)_2$ has an expanded cavity with dimensions of 2.97 × 11.42 Å as a consequence of an Fe–Fe bond character change. The Fe1–Fe1^i and Fe2–Fe2^i diagonal distances in the rectangular structure are approximately 11.66 and 11.80 Å for $4(BF_4)_4$ and $4(BF_4)_2$, respectively. The results of crystallographic analyses of the crystal structures of $4(BF_4)_4$ and $4(BF_4)_2$ show that upon reduction the bridging 1,4-diisocyanobenzene ligand bends inward toward the coordination of iron–sulfur core and the two benzene rings have nearly an eclipsed conformation. Additionally, the nonbonding distance between the two opposite benzene centers (the middle distance of the rectangular cavity) is 4.274 Å in $4(BF_4)_4$ and 3.782 Å in $4(BF_4)_2$, values that are longer than those of the rectangle side Fe–Fe distances of 2.6596(11) and 2.9706(8) Å, respectively. These structural comparisons indicate that expansion of the rectangular cavity is a consequence of a rectangular edge Fe–Fe distance change.

Magnetic Study of $4(BF_4)_2$. NMR investigation of $4(BF_4)_2$ shows that it exhibits paramagnetic behavior. The temperature dependence of the experimental molar magnetic susceptibility (χ_M) and $\chi_M T$ of $4(BF_4)_2$ has been investigated in order to understand its magnetic properties (Figure 7). The results show that the $\chi_M T$ value gradually decreases from 1.52 cm^3 K mol^{-1} at 300 K to 0.70 cm^3 K mol^{-1} at 10 K, at which point it rapidly decreases to 0.48 cm^3 K mol^{-1} at 2 K. The magnetic data of $4(BF_4)_2$ have been fitted to a one-J system, where the Hamiltonian is expressed as $H = -2JS_1 \cdot S_2$ and J is the magnetic exchange integral between two diiron units bridged by 1,4-diisocyaobenzene.[S7] The best fit (2–300 K) to the

dx.doi.org/10.1021/ic201380k | Inorg. Chem. 2011, 50, 10825–10834

Table 2. Selected Bond Lengths (Å) and Angles (deg) of $1(PF_6)_2$, $3(BF_4)_2$, $4(BF_4)_4$, and $4(BF_4)_2$ and Related Core Complexes $Fe_2(\mu\text{-SEt})_2$

complex		Fe−Fe	S−Fe−S	Fe−S−Fe	Fe−S	Fe−C	C−O	C−N	ref
$Cp_2Fe_2(\mu\text{-SEt})_2(CO)_2$	molecule 1	3.450(2)	79.2(1)	99.1(1)	2.263(2)	1.742(8)	1.144(14)		17
	molecule 2	3.415(2)	81.1(1)	97.2(1)	2.279(2)	1.751(8)	1.153(9)		
$[Cp_2Fe_2(\mu\text{-SEt})_2(CO)_2]^+$		2.957(4)	95.7(2)	82.8(2)	2.240(2)	1.71(1)	1.16(2)		19
$[Cp_2Fe_2(\mu\text{-SEt})_2(CN)(CNCH_3)]^+$		2.6372(10)	103.85(5), 103.53(5)	73.49(5) 2.2066(13), 2.2079(14)	2.2016(15), 2.2032(13)	1.914(6)[a]		1.139(7)[a]	30
						1.855(5)[b]		1.149(6)[b]	
$[Cp_2Fe_2(\mu\text{-SEt})_2(CNCH_3)_2]^{2+}$		2.6467(8)	102.49(4), 102.80(4)	73.66(4), 73.75(4) 2.2086(11), 2.2110(11)	2.1996(11), 2.2068(12)	1.867(4)		1.151(5)	30
						1.855(4)		1.148(5)	
$[Cp_2Fe_2(\mu\text{-SEt})_2(CO)_2]^{2+}$ ($\mathbf{1}^{2+}$)		2.6444(10)	103.66(5)	73.65(5), 73.65(5) 2.1961(15), 2.2009(14)	2.2111(15), 2.2159(15)	1.797(6)	1.123(6)		this work
			104.66(5)			1.804(6)	1.130(6)		
$[Cp_2Fe_2(\mu\text{-SEt})_2(1,4\text{-}CNC_6H_4NC)_2]^{2+}$ ($\mathbf{3}^{2+}$)		2.6309(11)	104.23(6)	73.30(5)	2.1876(15), 2.1981(15)	1.851(5)		1.138(6)[b]	this work
								1.139(6)[b]	
			105.53(6)	73.39(5)	2.2045(14), 2.2195(18)	1.836(5)		1.133(8)[c]	
								1.139(8)[c]	
$[Cp_4Fe_4(\mu\text{-SEt})_4(\mu\text{-}1,4\text{-}CNC_6H_4NC)_2]^{4+}$ ($\mathbf{4}^{4+}$)		2.6596(11)	104.24(6)	73.93(5)	2.2114(16), 2.2117(17)	1.830(6)		1.158(7)	this work
			104.37(6)	73.95(5)	2.2089(17), 2.2131(17)	1.843(6)		1.172(7)	
$[Cp_4Fe_4(\mu\text{-SEt})_4(\mu\text{-}1,4\text{-}CNC_6H_4NC)_2]^{2+}$ ($\mathbf{4}^{2+}$)		2.9706(8)	96.64(5)	82.88(4)	2.2437(12), 2.2450(13)	1.812(4)		1.162(5)	this work
			96.74(5)	82.97(4)	2.2412(12), 2.2432(12)	1.809(4)		1.165(5)	

[a]For Fe−CN. [b]For Fe−CNR. [c]For free CNR.

dx.doi.org/10.1021/ic201380k|*Inorg. Chem.* 2011, 50, 10825–10834

Table 3. Crystallographic Data for Iron–Sulfur Core Complexes $1(PF_6)_2$, $3(BF_4)_2$, $4(BF_4)_4$, and $4(BF_4)_2$

	$1[PF_6]_2$	$3[BF_4]_2$	$4[BF_4]_4{\cdot}4CH_3CN$	$4[BF_4]_2{\cdot}2CH_3CN$
empirical formula	$C_{16}H_{20}F_{12}Fe_2O_2P_2S_2$	$C_{30}H_{30}B_2F_8Fe_2N_4S_2$	$C_{52}H_{60}B_4F_{16}Fe_4N_8S_4$	$C_{48}H_{54}B_2F_8Fe_4N_6S_4$
fw	744.37	796.02	1495.96	1240.23
T (K)	200(2)	200(2)	200(2)	200(2)
cystal size (mm^3)	0.4 × 0.21 × 0.04	0.65 × 0.31 × 0.11	0.19 × 0.11 × 0.05	0.35 × 0.28 × 0.14
cryst syst	monoclinic	monoclinic	triclinic	orthorhombic
space group	$P2_1/n$	$P2_1/n$	$P\bar{1}$	*Pbca*
a (Å)	10.2360(2)	16.545(4)	9.9319(5)	14.1668(8)
b (Å)	13.4940(4)	10.091(3)	10.0189(6)	15.9170(8)
c (Å)	17.6290(4)	23.515(6)	16.4568(9)	23.6224(13)
α (deg)	90	90	89.470(4)	90°
β (deg)	90.0000(10)	94.328(4)	88.841(4)	90°
γ (deg)	90	90	72.603(3)	90°
V ($Å^3$)	2435.00(10)	3914.6(16)	1562.33(15)	5326.7(5)
Z	4	4	1	4
D_{calcd} (g cm^{-3})	1.937	1.351	1.590	1.547
μ (mm^{-1})	1.601	0.911	1.135	1.293
reflns measd/indep	14 284/4431	22 110/6901	10 478/5255	31 442/4676
data/restraints/params	4431/0/320	6901/01/430	5255/0/398	4676/0/327
GOF	1.168	1.088	1.029	1.047
R_{int}	0.1016	0.0501	0.0601	0.0426
R1 [$I > 2\sigma$] (all data)	0.0543 (0.0811)	0.0665 (0.0876)	0.0649 (0.0917)	0.0507 (0.0673)
wR2 [$I > 2\sigma$] (all data)	0.1397 (0.1775)	0.1998 (0.2127)	0.1705 (0.1846)	0.1381 (0.1496)
max peak/hole (e/$Å^3$)	1.146/−1.189	1.247/−0.603	1.587/−0.654	1.562/−0.872

Scheme 3. Representation of the Changes in the Fe–Fe Bond Distance and Fe–S–Fe Angle of Iron Thiolate Core Complexes in the Electrochemical Processes

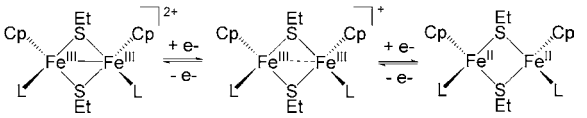

Fe-Fe distance: ~2.6 Å ~2.9 Å ~3.4 Å
Fe-S-Fe angle: ~99° ~83° ~74°
L= CO, CN⁻, CNR, CH_3CN, PR_3 ...

theoretical model corresponds to $g = 2.04$, $2J = -2.1$ cm^{-1}, and $R^2 = 0.999$. This finding shows that the two diiron units in $4(BF_4)_2$ are weakly antiferromagnetically coupled, suggesting that it has a singlet ground state and a triplet excited state that is ca. 0.006 cal mol^{-1} higher in energy. The results arising from this magnetic study are consistent with those coming from density functional theory (DFT) calculations (see below), which indicate that the spin density of the highest occupied molecular orbital (HOMO) of $4(BF_4)_2$ is largely localized at the Fe centers and that little spin population exists on the

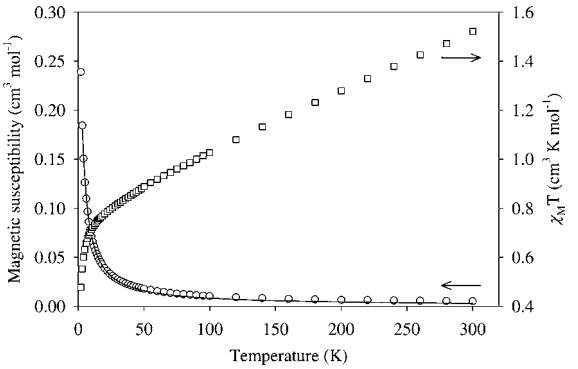

Figure 7. Plots of magnetic susceptibility (open circles) and $\chi_M T$ (open squares) versus temperature for complex $4(BF_4)_2$. The solid line is the best fit of the experimental data to the theoretical model.

diisocyanide bridges. The weak antiferromagnetic interaction is consistent with the proposal that the nonplanar configuration of Fe–CN–C_6H_4–NC–Fe reduces effective spin communication via a superexchange mechanism.

Scheme 4. Representation of the Redox Control Cavity Modulation of the Rectangular Tetranuclear Iron Thiolate Aryldiisocyanide Complex

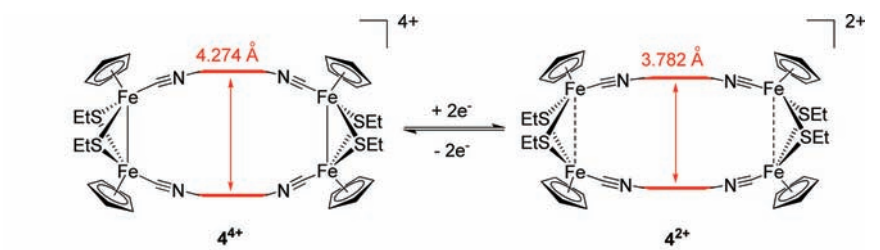

4^{4+} 4^{2+}
Fe-Fe distance: 2.6596(11)Å 2.9706(8)Å
Fe-L-Fe distance: 11.354Å 11.417Å
Fe-S-Fe angle: 73.94(5)° 82.93(4)°

dx.doi.org/10.1021/ic201380k | *Inorg. Chem.* 2011, 50, 10825–10834

Computational Results. Unrestricted DFT (UDFT) calculations were performed in order to gain insight into the electronic properties of the iron−sulfur core $\{Cp_2Fe_2(\mu\text{-}SEt)_2\}$ in rectangular macrocycle complexes $\mathbf{4}^{4+}$ and $\mathbf{4}^{2+}$.

The results of the UDFT calculations show that the electronic ground state of complex $\mathbf{4}^{4+}$ is a singlet with a ca. 15.1 kcal mol^{-1} lower energy than the triplet excited state. On the other hand, the singlet and triplet states for $\mathbf{4}^{2+}$ are almost isoenergetic, with the singlet state being only 0.003 kcal mol^{-1} lower in energy than the triplet state. This finding matches closely that arising from the magnetic study described above. It should be noted that the results of DFT reflect the molecular properties of the solid-state structure at 0 K, which could be different from those coming from the room temperature solution-phase NMR measurements.

On the basis of the paramagnetic behavior revealed by the results of NMR studies, we use the triplet state wave function of $\mathbf{4}^{2+}$ to explain the reduction behavior of complex **4**. The frontier orbitals of the triplet of $\mathbf{4}^{2+}$ are displayed in Figure 8, and

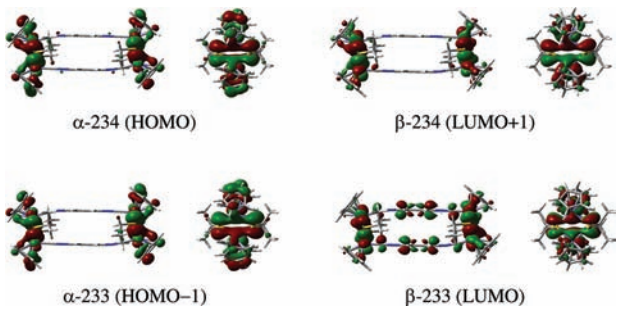

Figure 8. Frontier orbitals of the triplet of $\mathbf{4}^{2+}$.

Table 4. Population Analysis (%) of the Frontier Orbitals in the Triplet of $\mathbf{4}^{2+}$

MO	Fe atoms	S atoms	Cp rings	1,4-diisocyaobenzene
α-233	51	28	20	0
α-234	48	29	21	0
β-233	59	18	7	15
β-234	69	23	8	0

population analyses are shown in Table 4. Two important points arise from analysis of the frontier orbitals. First, it can be clearly seen that the α-occupied orbitals 233 and 234, which correspond to the HOMO−1 and HOMO, have antibonding character between two adjacent Fe atoms. This wave-function pattern is in agreement with the increase of the Fe−Fe distance occurring in the conversion of $\mathbf{4}^{4+}$ to $\mathbf{4}^{2+}$ that is revealed by the crystallographic data (cf. Table 2). Although the crystal structure of complex $\mathbf{4}^{0}$ is not available, the antibonding character between Fe atoms in β virtual orbitals 233 (lowest unoccupied molecular orbital, LUMO) and 234 (LUMO+1) in the triplet of $\mathbf{4}^{2+}$ suggests that a further increase in the Fe−Fe distance occurs when $\mathbf{4}^{2+}$ is reduced. Second, while the populations of the HOMO and HOMO−1 for $\mathbf{4}^{2+}$ are well separated and exclusively located on the two iron−sulfur cores $\{Cp_2Fe_2(\mu\text{-}SEt)_2\}$, the LUMO of $\mathbf{4}^{2+}$ obviously extends (ca. 15%) onto the 1,4-diisocyaobenzene bridge (cf. Figure 8 and Table 4). The observation that the HOMO and HOMO−1 of $\mathbf{4}^{2+}$ have no population on the 1,4-diisocyaobenzene bridge could indicate that the two diiron units are isolated from one another, a prediction that is in accordance with the observation of a single two-electron reductive peak from $\mathbf{4}^{4+}$ to $\mathbf{4}^{2+}$ in the CV. On the other hand, communication between the two subsequently added electrons is enhanced through delocalization of the wave function onto the bridge (see the β-233 LUMO for $\mathbf{4}^{2+}$), which corresponds to the observation of two distinguishable one-electron reduction peaks separated by 0.094 V for the third and fourth reduction steps.

SUMMARY AND CONCLUSIONS

The goal of this study was to explore the stepwise formation and self-assembly of supramolecular complexes derived from organometallic half-sandwich iron thiolate core complexes $\{Cp_2Fe_2(\mu\text{-}SEt)_2\}$ that contain the bridging 1,4-diisocyanobenzene ligand. This effort led to the preparation of an unusual rectangular tetranuclear iron thiolate core complex $[Cp_4Fe_4(\mu\text{-}SEt)_4(\mu\text{-}1,4\text{-}CNC_6H_4NC)_2](BF_4)_4$ ($\mathbf{4}(BF_4)_4$) by a self-assembly reaction between $[Cp_2Fe_2(\mu\text{-}SEt)_2(CH_3CN)_2](BF_4)_2$ ($\mathbf{2}(BF_4)_2$) and equimolar amounts of 1,4-diisocyanobenzene or by stepwise formation via the mixing of complex $\mathbf{2}[BF_4]_2$ and $[Cp_2Fe_2(\mu\text{-}SEt)_2(1,4\text{-}CNC_6H_4NC)_2](BF_4)_2$ ($\mathbf{3}(BF_4)_2$). Reversible reduction of rectangular tetranuclear iron−sulfur core complex $\mathbf{4}(BF_4)_4$ was found to take place first by a two-electron process and then via two separate one-electron steps. Isolation of the reduction product $\mathbf{4}(BF_4)_2$ has served to facilitate determination of the electrochemical behavior of the rectangular tetranuclear iron thiolate core complex. The detailed information about the solution electrochemical behavior of $\mathbf{3}(BF_4)_2$ and $\mathbf{4}(BF_4)_4$ that has come from this investigation should benefit efforts directed toward understanding the related electronchemical activities and complexation features of metal-containing supramolecules. Comparisons of the structures of the iron thiolate core $\{Cp_2Fe_2(\mu\text{-}SEt)_2\}$ in the rectangular macrocycle complexes $\mathbf{4}(BF_4)_4$ and $\mathbf{4}(BF_4)_2$ reveal that cavity changes occur as a result of redox control associated with one-electron and two-electron Fe−Fe bond formation. In addition, a crystallographic study of the rare ferric carbonyl complex $\mathbf{1}(PF_6)_2$ has yielded different results in comparison with those of well-known ferrous carbonyl analogues, which provide an excellent example demonstrating that the CO ligand has different π-back-bonding abilities that depend on the oxidation state of the metal center.

EXPERIMENTAL SECTION

All manipulations were carried out under an atmosphere of purified dinitrogen with standard Schlenk techniques. Chemical reagents were purchased from Aldrich Chemical Co. Ltd., Lancaster Chemicals Ltd., or Fluka Ltd. All of the reagents were used without further purification, apart from all solvents that were dried over sodium (Et_2O and THF) or CaH_2 (CH_2Cl_2 and CH_3CN) and then thoroughly degassed before use. $Cp_2Fe_2(\mu\text{-}SEt)_2(CO)_2$ and 1,4-diisocyanobenzene were prepared according to literature procedures.[29,58] IR spectra were recorded on a Varian 640 FT-IR spectrometer. ^1H and ^{13}C NMR spectra were acquired on a Varian Gemini-200, a Bruker Avance DRX-300, or a Varian VNMRS-600 NMR spectrometer. ESI-MS spectra were collected on a Waters ZQ 4000 or a Varian 901-MS (FT-ICR) mass spectrometer. Elemental analyses were performed on a Heraeus CHN-OS Rapid elemental analyzer. CV was measured at a scan rate of 100 mV s^{-1} at around 10^{-4} M MeCN solutions using 0.1 M $(Bu_4N)(PF_6)$ as the supporting electrolyte and referenced to $Fc^{+/0}$. A platinum wire counter electrode, a glassy carbon working electrode, and an Ag/AgCl (MeCN) reference electrode were used.

dx.doi.org/10.1021/ic201380k | Inorg. Chem. 2011, 50, 10825−10834

$[Cp_2Fe_2(\mu\text{-SEt})_2(CO)_2](BF_4)_2$ [1$(BF_4)_2$]. The preparation method is similar to that described by the literature.[25] A solution containing an excess of bromine (1.44 g, 9.01 mmol) in dichloromethane was added dropwise to a stirred solution of the complex $Cp_2Fe_2(\mu\text{-SEt})_2(CO)_2$ (2.52 g, 6.00 mmol) and excess NH_4BF_4 (3.85 g, 36.72 mmol; in a minimum amount of methanol) in dichloromethane at room temperature. The green product that precipitated from the solution was washed thoroughly with benzene and a small amount of dichloromethane. Yield: 2.85 g (80%). X-ray-quality crystals were obtained by the slow diffusion of ether into a methanol solution of the PF_6^- salt at −20 °C. IR (CH_3CN, cm^{-1}): ν_{CO} 2071 (s), 2059 (m). UV−vis [CH_3CN; λ/nm (ε/M^{-1} cm^{-1})]: 207 (9650), 234 (5740), 333 (2038), 607 (435). ESI-MS(+): 212.00 (15%; $[Cp_2Fe_2(\mu\text{-SEt})_2(CO)]^{2+}$), 419.90 (100%; $[Cp_2Fe_2(\mu\text{-SEt})_2(CO)_2 + H]^+$).

$[Cp_2Fe_2(\mu\text{-SEt})_2(CH_3CN)_2](BF_4)_2$ [2$(BF_4)_2$]. A mixture of 2.85 g (4.80 mmol) of $[Cp_2Fe_2(\mu\text{-SEt})_2(CO)_2](BF_4)_2$ and 4.00 g (38.15 mmol) of NH_4BF_4 was refluxed in 70 mL of CH_3CN in a round-bottomed flask with a condenser open to air. After 6 h of refluxing, the mixture was reduced in volume to about 8 mL, and the addition of 50 mL of H_2O precipitated the product $[Cp_2Fe_2(\mu\text{-SEt})_2(CH_3CN)_2](BF_4)_2$. The product was washed with 20 mL of H_2O. Redissolving the initial product in 70 mL of CH_3CN and slowly reducing the solvent in rotavapor gave a pure black microcrystalline product. Yield: 1.84 g (62%). IR (CH_3CN, cm^{-1}): ν_{CN} 2295 (s). UV−vis [CH_3CN; λ/nm (ε/M^{-1} cm^{-1})]: 213 (5502), 243 (4997), 337 (2536), 407 (1124). ^1H NMR (CD_3CN): δ 1.73 (t, J_{H-H} = 3.8 Hz, 6H, CH_3CH_2S), 1.95 (s, $NCCH_3$), 2.75 (quartet, J_{H-H} = 3.8 Hz, 4H, CH_3CH_2S), 5.35 (s, 10H, C_5H_5). ESI-MS(+): 223.01 ($[Cp_2Fe_2(\mu\text{-SEt})_2(NCCH_3)_2]^{2+}$).

$[Cp_2Fe_2(\mu\text{-SEt})_2(1,4\text{-}CNC_6H_4NC)_2](BF_4)_2$ [3$(BF_4)_2$]. To a solution of 2$(BF_4)_2$ (124 mg, 0.20 mmol) in 10 mL of CH_3CN was added 1,4-diisocyanobenzene (256 mg, 2.00 mmol) dissolved in 10 mL of CH_3CN. The solution was stirred for 10 min under an inert atmosphere. The solvent was evaporated under vacuum and the residue washed with ether to give a yellow-green solid. The solid was dried under vacuum. Yield: 155 mg (98%). Anal. Calcd. for $C_{30}H_{28}B_2F_8Fe_2N_2S_2$: C, 45.38; H, 3.55; N, 7.06. Found: C, 45.45; H, 3.51; N, 7.09. IR (CH_3CN, cm^{-1}): ν_{CN} 2164 (s), 2128 (m). UV−vis [CH_3CN; λ/nm (ε/M^{-1} cm^{-1})]: 241 (48 586), 291 (23 149), 341 (17 368), 633 (694). ^1H NMR (CD_3CN): δ 1.72 (t, J_{H-H} = 3.8 Hz, 6H, CH_3CH_2S), 3.02 (quartet, J_{H-H} = 3.8 Hz, 4H, CH_3CH_2S), 5.71 (s, 10H, C_5H_5), 7.29 (d, J_{H-H} = 9 Hz, 4H, C_6H_4), 7.47 (d, J_{H-H} = 9 Hz, 4H, C_6H_4). $^{13}C\{^1H\}$ NMR (CD_3CN): δ 17.64 (s, SCH_2CH_3), 43.43 (s, SCH_2CH_3), 94.10 (C_5H_5), 128.99 (s, C_6H_4), 158.09 (s, Fe(1,4-CNC_6H_4NC)), 168.86 (s, Fe(1,4-CNC_6H_4NC)). ESI-MS(+): 246.14 (80%; $[Cp_2Fe_2(\mu\text{-SEt})_2(1,4\text{-CN-}C_6H_4NC)]^{2+}$), 310.04 (100%; $[Cp_2Fe_2(\mu\text{-SEt})_2(1,4\text{-CN-}C_6H_4NC)_2]^{2+}$), 706.9 (20%; $[Cp_2Fe_2(\mu\text{-SEt})_2(1,4\text{-CN-}C_6H_4NC)_2(BF_4)]^+$).

$[Cp_4Fe_4(\mu\text{-SEt})_4(\mu\text{-}1,4\text{-}CNC_6H_4NC)_2](BF_4)_4$ [4$(BF_4)_4$]. *Method A.* To a solution of 3$(BF_4)_2$ (159 mg, 0.20 mmol) in 10 mL of CH_3CN was added 2$(BF_4)_2$ (124 mg, 0.20 mmol) dissolved in 10 mL of CH_3CN. The solution was stirred for 24 h under a N_2 atmosphere to afford yellow-green microcrystals of the product. Microcrystal 4$(BF_4)_4$ was collected on a glass frit and dried under vacuum. Yield: 218 mg (82%). Anal. Calcd. for $C_{44}H_{48}B_4F_{16}Fe_4N_4S_4$: C, 39.68; H, 3.63; N, 4.21. Found: C, 39.48; H, 3.71; N, 4.20. IR (CH_3CN, cm^{-1}): ν_{CN} 2156 (s). UV−vis [CH_3CN; λ/nm (ε/M^{-1} cm^{-1})]: 242 (52 715), 325 (28 732), 630 (1335). ^1H NMR (CD_3CN): δ 1.91 (t, J_{H-H} = 7.2 Hz, 6H, CH_3CH_2S), 3.15 (quartet, J_{H-H} = 7.2 Hz, 4H, CH_3CH_2S), 5.70 (s, 10H, C_5H_5), 6.96(s, 8H, C_6H_4). $^{13}C\{^1H$ NMR (CD_3CN): δ 17.61 (s, SCH_2CH_3), 41.65 (s, SCH_2CH_3), 93.93 (C_5H_5), 128.85 (s, C_6H_4). ESI-MS(+): 246.05 ($[Cp_4Fe_4(\mu\text{-SEt})_4(\mu\text{-}1,4\text{-}CNC_6H_4NC)_2]^{4+}$).

Method B. A solution of 2$(BF_4)_2$ (124 mg, 0.20 mmol) and 1,4-diisocyanobenzene (26 mg, 0.20 mmol) in 20 mL of CH_3CN was stirred for 24 h under a N_2 atmosphere to afford yellow-green microcrystals of the product. Microcrystals 4$(BF_4)_4$ were collected on a glass frit and dried under vacuum. Yield: 88 mg (66%).

Chemical Reduction of 4$(BF_4)_4$. To a well-stirred solution of 4$(BF_4)_4$ (100 mg, 0.08 mmol) in 200 mL of CH_3CN was added KC_8 (22 mg, 0.16 mmol). The solution, which was initially yellow-green, became a very dark-green color. After 5 min, all of KC_8 appeared to have been consumed, and the slurry was filtered through Celite. The CH_3CN solvent was evaporated under vacuum, and the residue washed with ether. The green solid of 4$(BF_4)_2$ was dried under vacuum. Yield: 81 mg (70%). Anal. Calcd for $C_{44}H_{48}B_2F_8Fe_4N_4S_4$: C, 45.63; H, 4.18; N, 4.84. Found: C, 45.52; H, 4.11; N, 4.89. IR (CH_3CN, cm^{-1}): ν_{CN} 2097 (s). UV−vis [CH_3CN; λ/nm (ε/M^{-1} cm^{-1})]: 253 (35 003), 357 (19 355), 631 (2784). ESI-MS(+): 491.94 (100%; $[Cp_4Fe_4(\mu\text{-SEt})_4(1,4\text{-CN-}C_6H_4NC)_2]^{2+}$), 309.93 (20%; $[Cp_2Fe_2(\mu\text{-SEt})_2(1,4\text{-CN-}C_6H_4NC)_2(BF_4)]^+$).

X-ray Crystal Structure Determination. Single crystals of complex 1$(PF_6)_2$ suitable for X-ray analysis were obtained by diffusion of Et_2O into a CH_3OH solution. Crystal samples of complexes 3$(BF_4)_2$, 4$(BF_4)_4$, and 4$(BF_4)_2$ were grown from a concentrated CH_3CN solution or by diffusion of Et_2O into a CH_3CN solution at −20 °C. All single-crystal X-ray diffraction data were measured on a Bruker Nonius Kappa CCD diffractometer using λ(Mo Kα) radiation (λ = 0.710 73 Å). Data collection was executed using the *SMART* program.[59] Cell refinement and data reduction were made with the *SAINT* program.[60] The structure was determined using the *SHELXTL/PC* program[61] and refined using full-matrix least squares. All non-H atoms were refined anisotropically, whereas H atoms were placed at calculated positions and included in the final stage of refinement with fixed parameters. The disordered CH_3CN and ether solvent molecules in complex 4$(BF_4)_2$ were removed from the diffraction data using the *SQUEEZE* program. A summary of the relevant crystallographic data for complexes 1$(PF_6)_2$, 3$(BF_4)_2$, 4$(BF_4)_4$, and 4$(BF_4)_2$ is provided in Table 3.

Magnetic Measurements. The magnetic data of complex 4$(BF_4)_2$ were recorded on a SQUID magnetometer (SQUID-VSM, Quantum Design) under an external magnetic field (1 T) in the temperature range of 2−300 K. The magnetic susceptibility data were corrected with ligand diamagnetism by the tabulated Pascal's constants.

Computational Methods. Single-point energy calculations using DFT were carried out for the crystal structures of complexes 4^{4+} and 4^{2+} to shed some light on the nature of the electronic structures. The combination of the hybrid functional B3LYP with 6-31+G* basis sets for H, C, N, and S atoms and the Stuttgart pseudopotental and complementary basis set (SDDALL keyword in the *Gaussian 09* program) for Fe atoms was employed in these calculations. To investigate which spin state, singlet or triplet, is the electronic ground state and responsible for experimental observation, both spin states for complexes 4^{4+} and 4^{2+} were calculated by the unrestricted wave-function method. The stability of the wave functions was tested (Stable=Opt keyword in the *Gaussian 09* program). Calculations were performed by the *Gaussian 09* program,[62] and the frontier orbitals were displayed by *GaussView* graphical interface.[63]

■ ASSOCIATED CONTENT

Ⓢ Supporting Information

Additional figures (Figures S1−S11) and Table S1 and crystallographic data in CIF format for the structural determinations of 1$(PF_6)_2$, 3$(BF_4)_2$, 4$(BF_4)_4$, and 4$(BF_4)_2$. This material is available free of charge via the Internet at http://pubs.acs.org.

■ AUTHOR INFORMATION

Corresponding Author

*E-mail: sodiohsu@kmu.edu.tw.

■ ACKNOWLEDGMENTS

Financial support of the National Science Council (Taiwan) is highly appreciated. We thank the National Center for High-Performance Computing for computer time and facilities.

REFERENCES

(1) Lee, S. J.; Lin, W. *Acc. Chem. Res.* **2008**, *41*, 521.
(2) Amijs, C. H. M.; van Klink, G. P. M.; van Koten, G. *Dalton Trans.* **2006**, 308.
(3) Thanasekaran, P.; Liao, R.-T.; Liu, Y.-H.; Rajendran, T.; Rajagopal, S.; Lu, K.-L. *Coord. Chem. Rev.* **2005**, *249*, 1085.
(4) Würthner, F.; You, C.-C.; Saha-Möller, C. R. *Chem. Soc. Rev.* **2004**, *33*, 133.
(5) Dinolfo, P. H.; Hupp, J. T. *Chem. Mater.* **2001**, *13*, 3113.
(6) Leininger, S.; Olenyuk, B.; Stang, P. J. *Chem. Rev.* **2000**, *100*, 853.
(7) Rauchfuss, T. B.; Severin, K. In *Organic Nanostructures*; Atwood, J., Steed, J., Eds.; Wiley-VCH: New York, 2008; p 179.
(8) Klausmeyer, K. K.; Rauchfuss, T. B.; Wilson, S. R. *Angew. Chem., Int. Ed.* **1998**, *37*, 1694.
(9) Han, Y.-F.; Jia, W.-G.; Yu, W.-B.; Jin, G.-X. *Chem. Soc. Rev.* **2009**, *38*, 3419.
(10) Zhang, W.-Z.; Han, Y.-F.; Lin, Y.-J.; Jin, G.-X. *Organometallics* **2010**, *29*, 2842.
(11) Yu, W.-B.; Han, Y.-F.; Lin, Y.-J.; Jin, G.-X. *Organometallics* **2010**, *29*, 2827.
(12) Venkateswara, R. P.; Holm, R. H. *Chem. Rev.* **2004**, *104*, 527.
(13) Fontecilla-Camps, J. C.; Volbeda, A.; Cavazza, C.; Nicolet, Y. *Chem. Rev.* **2007**, *107*, 4273.
(14) Madec, P.; Muir, K. W.; Pétillon, F. Y.; Rumin, R.; Scaon, Y.; Schollhammer, P.; Talarmin, J. *J. Chem. Soc., Dalton Trans.* **1999**, 2371.
(15) Büchner, R.; Field, J. S.; Haines, R. J. *J. Chem. Soc., Dalton Trans.* **1997**, 2403.
(16) Büchner, R.; Field, J. S.; Haines, R. J. *J. Chem. Soc., Dalton Trans.* **1996**, 3533.
(17) Toshev, M. T.; Dustov, K. B.; Nekhaev, A. I.; Aleksandrov, G. G.; Alekseeva, S. D.; Kolobkov, B. I. *Koord. Khim.* **1991**, *17*, 930.
(18) Gaete, W.; Ros, J.; Yanez, R.; Solans, X.; Font-Altaba, M. *J. Organomet. Chem.* **1986**, *316*, 169.
(19) English, R. B. *Acta Crystallogr.* **1984**, *C40*, 1567.
(20) Kubas, G. J.; Vergamini, P. J. *Inorg. Chem.* **1981**, *20*, 2667.
(21) Vergamini, P. J.; Kubas, G. J. *Prog. Inorg. Chem.* **1976**, *21*, 261.
(22) Watkins, D. D. Jr.; George, T. A. *J. Organomet. Chem.* **1975**, *102*, 71.
(23) Haines, R. J.; de Beer, J. A.; Greatrex, R. *J. Organomet. Chem.* **1975**, *85*, 89.
(24) Frisch, P. D.; Lloyd, M. K.; McCleverty, J. A.; Seddon, D. *J. Chem. Soc., Dalton Trans.* **1973**, 2268.
(25) de Beer, J. A.; Haines, R. J.; Greatrex, R.; van Wyk, J. A. *J. Chem. Soc., Dalton Trans.* **1973**, 2341.
(26) Clare, M.; Hill, H. A. O.; Johnson, C. E.; Richards, R. *J. Chem. Soc., Dalton Trans.* **1970**, 1376.
(27) Connelly, N. G.; Dahl, L. F. *J. Am. Chem. Soc.* **1970**, *92*, 7472.
(28) Ferguson, G.; Hannaway, C.; Islam, K. M. S. *Chem. Commun.* **1968**, 1165.
(29) King, R. B.; Bisnette, M. B. *Inorg. Chem.* **1965**, *4*, 482.
(30) Hsu, S. C. N.; Zheng, Y.-C.; Chen, H.-Y.; Hung, M.-Y.; Kuo, T.-S. *J. Organomet. Chem.* **2008**, *693*, 3035.
(31) Shi, C.-C.; Chen, C.-S.; Hsu, S. C. N.; Yeh, W.-Y.; Chiang, M. Y.; Kuo, T.-S. *Inorg. Chem. Commun.* **2008**, *11*, 1264.
(32) Hsu, S. C. N.; Chen, H. H. Z.; Lin, I.-J.; Liu, J.-J.; Chen, P.-Y. *J. Organomet. Chem.* **2007**, *692*, 3676.
(33) Hsu, S. C. N.; Chien, S. S. C.; Chen, H. H. Z.; Chiang, M. Y. *J. Chin. Chem. Soc.* **2007**, *54*, 685.
(34) Irwin, M. J.; Rendina, L. M.; Vittal, J. J.; Puddephatt, R. J. *Chem. Commun.* **1996**, 1281.
(35) Suzuki, H.; Tajima, N.; Tatsumi, K.; Yamamoto, Y. *Chem. Commun.* **2000**, 1801.
(36) Yamamotoa, Y.; Suzuki, H.; Tajima, N.; Tatsumi, K. *Chem.—Eur. J.* **2002**, *8*, 372.
(37) Huang, J.; Lin, R.; Wu, L.; Zhao, Q.; Zhu, C.; Wen, T. B.; Xia, H. *Organometallics* **2010**, *29*, 2916.
(38) Contakes, S. M.; Hsu, S. C. N.; Rauchfuss, T. B.; Wilson, S. R. *Inorg. Chem.* **2002**, *41*, 1670.
(39) Bley, B.; Willner, H.; Aubke, F. *Inorg. Chem.* **1997**, *36*, 158.
(40) Hsu, H.-F.; Koch, S. A.; Popescu, C. V.; Münck, E. *J. Am. Chem. Soc.* **1997**, *119*, 8371.
(41) Delville-Desbois, M.-H.; Mross, S.; Astruc, D.; Linares, J.; Varret, F.; Rabaâ, H.; Beuze, A. L.; Saillard, J.-Y.; Culp, R. D.; Atwood, D. A.; Cowley, A. H. *J. Am. Chem. Soc.* **1996**, *118*, 4133.
(42) Etzenhouser, B. A.; Cavanaugh, M. D.; Spurgeon, H. N.; Sponsler, M. B. *J. Am. Chem. Soc.* **1994**, *116*, 2221.
(43) Morrow, J.; Catheline, D.; Desbois, M. H.; Manriquez, J. M.; Ruiz, J.; Astruc, D. *Organometallics* **1987**, *6*, 2605.
(44) Evans, D. F. *J. Chem. Soc.* **1959**, 2003.
(45) Schubert, E. M. *J. Chem. Educ.* **1992**, *69*, 62.
(46) Reedy, B. J.; Murthy, N. N.; Karlin, K. D.; Blackburn, N. J. *J. Am. Chem. Soc.* **1995**, *117*, 9826.
(47) Guy, M. P.; Guy, J. T.; Bennett, D. W. *Organometallics* **1986**, *5*, 1696.
(48) Grubisha, D. S.; Rommel, J. S.; Lane, T. M.; Tysoe, W. T.; Bennett, D. W. *Inorg. Chem.* **1992**, *31*, 5022.
(49) Rommel, J. S.; Weinrach, J. B.; Grubisha, D. S.; Bennett, D. W. *Inorg. Chem.* **1988**, *27*, 2945.
(50) Han, Y.-F.; Lin, Y.-J.; Jia, W.-G.; Jin, G.-X. *Organometallics* **2008**, *27*, 4088.
(51) Boyer, J. L.; Ramesh, M.; Yao, H.; Rauchfuss, T. B.; Wilson, S. R. *J. Am. Chem. Soc.* **2007**, *129*, 1931.
(52) O'Dea, J. J.; Osteryoung, J.; Osteryoung, R. A. *J. Phys. Chem.* **1983**, *87*, 3911.
(53) Hartmann, H.; Berger, S.; Winter, R.; Fiedler, J.; Kaim, W. *Inorg. Chem.* **2000**, *39*, 4977.
(54) Kaim, W.; Schwederski, B.; Dogan, A.; Fiedler, J.; Kuehl, C. J.; Stang, P. J. *Inorg. Chem.* **2002**, *41*, 4025.
(55) Richardson, D. E.; Taube, H. *J. Am. Chem. Soc.* **1983**, *105*, 40.
(56) Shaik, S.; Hoffmann, R.; Fisel, C. R.; Summerville, R. H. *J. Am. Chem. Soc.* **1980**, *102*, 4555.
(57) Bleaney, B.; Bowers, K. D. *Proc. R. Soc. London, Ser. A* **1952**, *214*, 451.
(58) Wagner, N. L.; Murphy, K. L.; Haworth, D. T.; Bennett, D. W. *Inorg. Synth.* **2004**, *34*, 24.
(59) Sheldrick, G. M. *SHELXL-97, Program for the Refinement of Crystal Structures*; University of Göttingen: Göttingen, Germany, 1997.
(60) *SAINT Manual*, version 5/6.0; Bruker Analytical X-ray Systems Inc.: Madison, WI, 1997.
(61) Sheldrick, G. M. *SHELXL-97, Program for the Refinement of Crystal Structures*; University of Göttingen: Göttingen, Germany, 1997.
(62) Frisch, M. J.; Trucks, G. W.; Schlegel, H. B.; Scuseria, G. E.; Robb, M. A.; Cheeseman, J. R.; Scalmani, G.; Barone, V.; Mennucci, B.; Petersson, G. A.; Nakatsuji, H.; Caricato, M.; Li, X.; Hratchian, H. P.; Izmaylov, A. F.; Bloino, J.; Zheng, G.; Sonnenberg, J. L.; Hada, M.; Ehara, M.; Toyota, K.; Fukuda, R.; Hasegawa, J.; Ishida, M.; Nakajima, T.; Honda, Y.; Kitao, O.; Nakai, J.; Vreven, T.; Montgomery, J. A., Jr.; Peralta, J. E.; Ogliaro, F.; Bearpark, M.; Heyd, J. J.; Brothers, E.; Kudin, K. N.; Staroverov, V. N.; Kobayashi, R.; Normand, J.; Raghavachari, K.; Rendell, A.; Burant, J. C.; Iyengar, S. S.; Tomasi, J.; Cossi, M.; Rega, N.; Millam, J. M.; Klene, M.; Knox, J. E.; Cross, J. B.; Bakken, V.; Adamo, C.; Jaramillo, J.; Gomperts, R.; Stratmann, R. E.; Yazyev, O.; Austin, A. J.; Cammi, R.; Pomelli, C.; Ochterski, J. W.; Martin, R. L.; Morokuma, K.; Zakrzewski, V. G.; Voth, G. A.; Salvador, P.; Dannenberg, J. J.; Dapprich, S.; Daniels, A. D.; Farkas, O.; Foresman, J. B.; Ortiz, J. V.; Cioslowski, J.; Fox, D. J. *Gaussian 09*; Gaussian, Inc.: Wallingford, CT, 2009.
(63) Dennington, R.; Keith, T.; Millam, J. *GaussView*; Semichem Inc.: Shawnee Mission, KS, 2009.